Valveless Pulsejet Engine

A Senior Project

presented to

the Faculty of the Aerospace Engineering Department

California Polytechnic State University, San Luis Obispo

In Partial Fulfillment

of the Requirements for the Degree

Bachelor of Science Aerospace Engineering

by

Cory Kerr and James Reynolds

June 2010

Progress Report – Pulsejet Engine

Cory Kerr[1] and James Reynolds[1]
California Polytechnic State University, San Luis Obispo, CA 93407

The goal of this project is to build a valveless pulsejet based on the Lady Anne model, known as the Focused Wave Engine VIII Twin Stack. This project has two main goals. The first goal is to design and build the valveless pulsejet. This includes machine work on stainless steel to build the engine, as well as modifying copper tubes to serve as a fuel injection system. The second goal is to build a test stand that allows for accurate data collection of the total thrust being produced by the engine and acts as a fuel injection and ignition system. The pulsejet design was found to produce upwards of 4 lbs of thrust at optimum fuel to air ratios.

Nomenclature

Symbol

A	=	area
a	=	acceleration
F	=	force
$\dot{m}$	=	mass flow rate
P	=	pressure

Subscripts

1	=	leading edge of pressure wave
2	=	trailing edge of pressure wave
dif	=	difference

I. Introduction

The aim of this project is to design and build a valveless pulsejet engine, and then to proceed to testing this pulsejet engine that could be potentially used as a learning tool for undergraduate courses in the Aerospace Engineering department at Cal Poly.

A variation on the Lady Anne model, known as the Focused Wave Engine (FWE) VIII Twin Stack was chosen for the design of this engine. The engine is built out of stainless steel 304 and uses a fuel injection system composed of modified copper tubing. The ideal test apparatus consists of thermal couples and pressure transducers placed in the combustion chamber and at the inlets and the exhaust nozzle, with the purpose of measuring temperature and pressure differences at the areas of interest on the pulsejet. Although for the experiment the only instrumentation available was a load cell in the test stand to measure the thrust produced by the engine.

II. Background

A. Definition

A pulsejet is a simple form of an air breathing jet engine that has few or no moving parts. The pulsejet acts in cycles, or pulses, where air is drawn into a combustion chamber, mixed with fuel, ignited, and then accelerated out of a nozzle providing thrust.

There are two basic categories of a pulsejet engine. The first is a valved design, in which the combustion process is controlled by valves. The air passes through these valves, and then when combustion begins, the valves slam shut, forcing the combustion products to exit through the nozzle, providing forward thrust. This type of engine requires more parts for the valved system, which results in potential for more problems.

[1] Undergraduate Student, Aerospace Engineering Department, 1 Grand Ave, and AIAA Student Member.

The second category of pulsejets is known as a valveless system, in which the valved system is completely removed. This results in the valveless designs having no moving parts, resulting in an engine that is easier to construct and maintain. Valveless pulsejets have three basic parts: the intake tubes, combustion chamber, and exhaust nozzle. When combustion occurs, the intake tubes attempt to limit the expulsion of combustion products, but do not stop it all together, as in the valved design. This means that while the majority of the combustion products exit the nozzle, a small part will exit from the intake. Because of this, many valveless designs have the intake facing in the same direction as the nozzle, to provide all thrust in the same direction.

B. Background

The first pulsejet was developed in 1906 by Russian engineer V.V. Karavodin. Soon after in 1908, French inventor Georges Marconnet patented the first valveless pulsejet design. This design helped influence the first significant application of a pulsejet, the Argus AS 109-014 valved pulsejet engine, developed by Paul Schmidt and the Argus Company of Germany.

The Argus AS 109-014 powered the *Vergeltungswaffe 1* (V-1) "buzz bomb", as seen in Fig. 1. This bomb and engine were used extensively by the Germans in World War II as the world's first cruise missile. The simplicity, low costs, and effectiveness of the design impressed the Allies, enough so that they began developing their own pulsejet designs.[1]

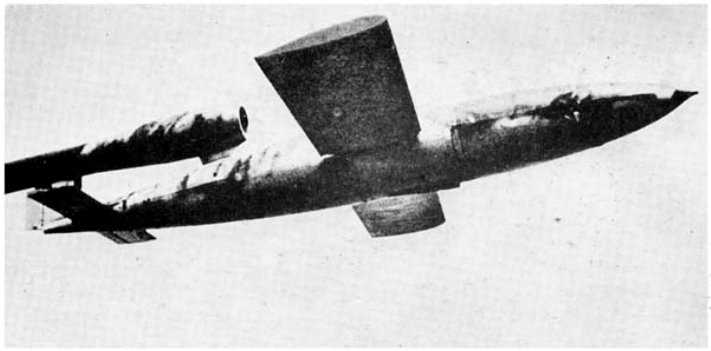

Figure 1. German V-1 "Buzz Bomb"[1]

Following the end of World War II, the US military put considerable research into development of a pulsejet engine of their own, but found that the turbojet engines were to be the engine of the future. This resulted in a considerable drop off into pulsejet research during the 1960's.

As recent as 1980, pulsejets were revitalized in the form of a hobbyist type jet engine. Since the pulsejets are relatively inexpensive, people interested in model aircraft propulsion began developing small pulsejet engines to power these vehicles. Since then, a large community of these hobbyists has developed over the internet, where most pulsejet innovation is found today.

As recent as 2006, the Russian company ENICS has used a pulsejet engine in UAV applications. Specifically the pulsejet is used in a UAV target drone, known as the E-95. The E-95 serves the purpose of simulating subsonic UAVs, cruise missiles, glide bombs, helicopters and attack aircraft. It is a significant development, since it marks the first military use of a pulsejet engine since WWII.

The FWE VIII Twin Stack design is based on the Chinese CS engine design, which is featured in Fig. 2. Developed in the 1950's by CS of Shanghai, the intake valve branches out from the combustion chamber at a 45 degree angle, and then turns again to face in the same direction as the exhaust nozzle. The Chinese CS design is considered one of the better pulsejet engine designs; however it requires careful attention to proportions to improve performance. The FWE VIII Twin Stack employs an additional intake valve on the opposite side, resulting in a twin intake configuration. In addition the FWE VIII Twin Stack uses converging diverging sections, as well as flared ends on the intake and nozzle, which theoretically leads to an increase in performance.

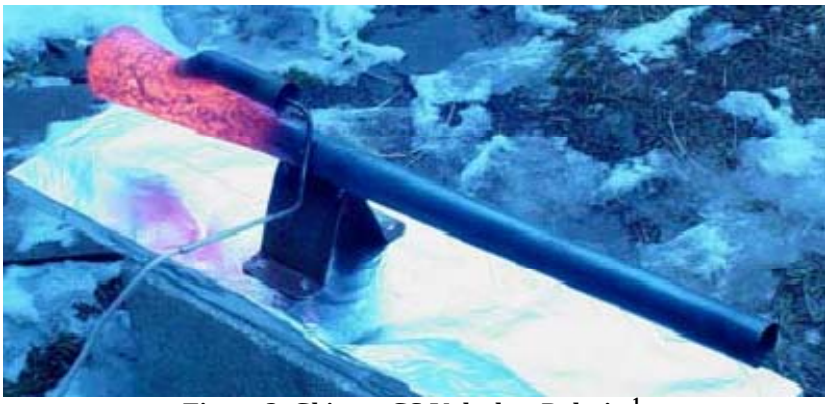

Figure 2. Chinese CS Valveless Pulsejet[1]

C. Operating Principle

To start, the common name of "valveless pulsejet" is a misnomer. While it certainly has no mechanical valves, nor any moving parts for that matter, it does have aerodynamic valves. The simplest of these consisting of an intake port that is smaller than the exhaust. The technical name for this type of pulsejet is acoustic-type pulsejet or aerodynamically valved pulsejet but will be referred to throughout this paper simply as a valveless pulsejet.

The valveless pulsejet is the simplest jet engine that can run statically. It is composed of three main components, the intake, combustion chamber and exhaust, as shown in Fig. 3.

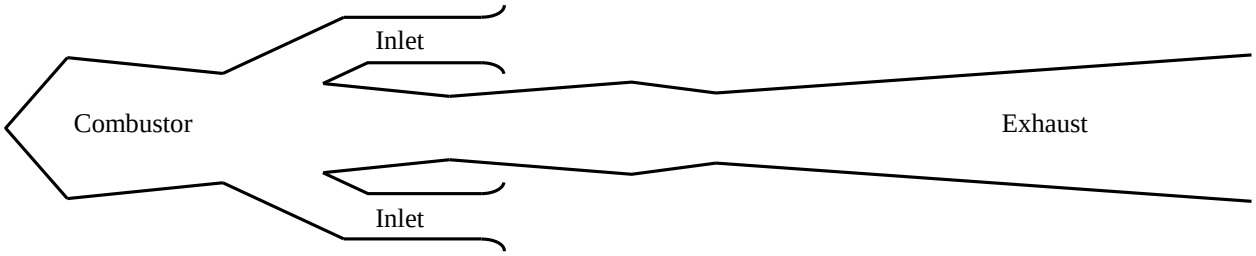

Figure 3. Components of a Valveless Pulsejet Engine

The following paragraphs will provide a walkthrough of the operational process using the legend shown in Fig. 4 where a dashed line is a compression wave, a dotted line is a rarefaction wave and the arrow indicates direction.

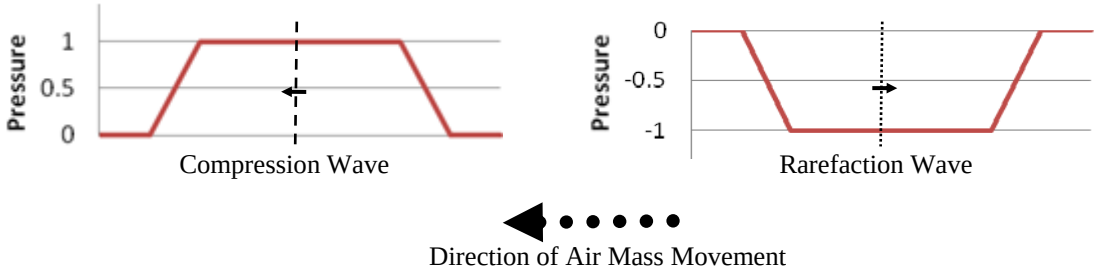

Figure 4. Operational Process Legend

The nonsteady, intermittent process begins with ignition of the fuel air mixture in the combustion chamber. This is technically deflagration and not an explosion. The difference lies in quickly burning verses detonation. The deflagration causes a rise in pressure in the combustion chamber and a compression wave. This compression wave travels down both the inlet and exhaust ducts, at the speed of sound. The heat addition of the deflagration causes the air mass to expand and begin flowing down the ducts. The smaller air mass of the inlet is rapidly accelerated outward behind the pressure wave while the larger exhaust duct reacts more slowly.[5] This process is depicted in Fig. 5.

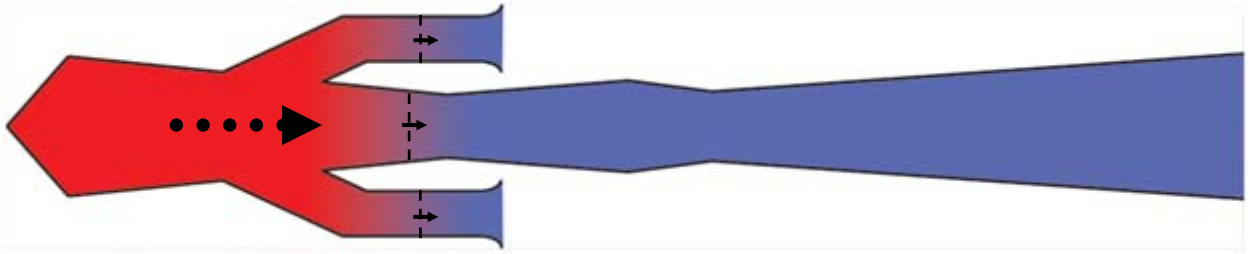

Figure 5. Beginning of Combustion Cycle, Compression Wave

When the compression wave reaches the end of each tube it is reflected in the opposite direction as a low pressure rarefaction wave. This happens first in the shorter, smaller inlet and then in the exhaust. The rarefaction wave in the inlet is relatively weak but the flow still reverses first in the inlet due to its smaller air mass and preloads it with fresh air. The hot combustion gases continue to flow down and out the exhaust duct even as the rarefaction wave travels back towards the combustion chamber, as seen in Fig. 6.

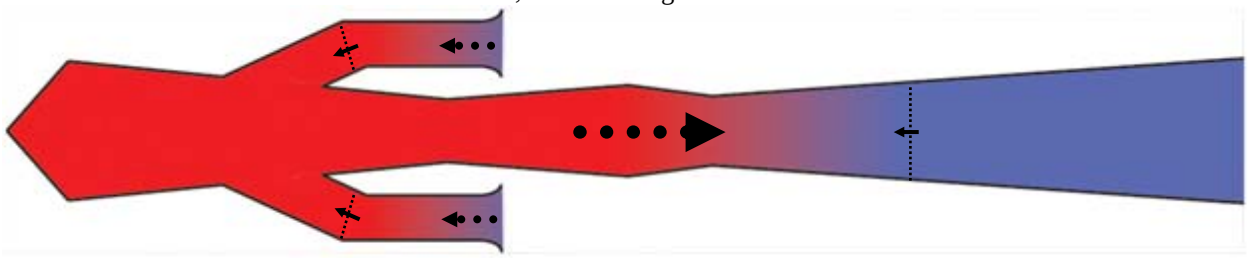

Figure 6. Reflection of Rarefaction Wave

The reduction of heat edition from the end of combustion and the arrival of the rarefaction wave in the combustor causes a pressure drop below ambient. Now the engine truly breathes and the fresh air is drawn in the inlet into the combustion chamber. The inertia of the exhaust gases kept them flowing out the exhaust even as air was already flowing in the inlet. The rarefaction wave is partially reflected from the end of the combustor and transmitted back towards the exhaust staying a rarefaction wave. The air in the exhaust just begins to change directions as seen in Fig. 7.

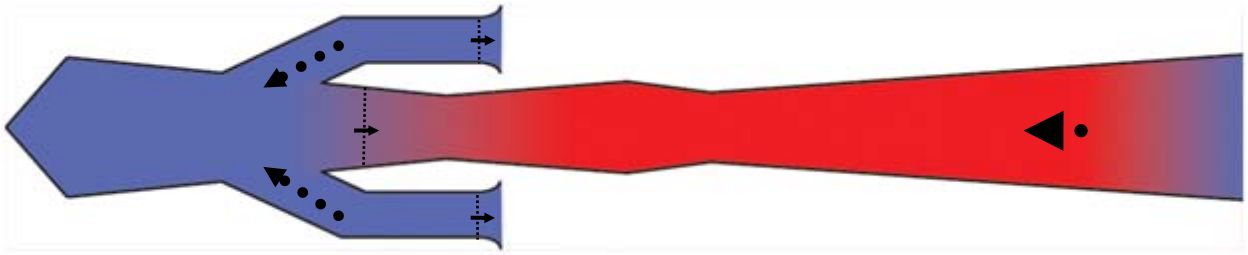

Figure 7. Second Reflection of Rarefaction Wave

The reflected rarefaction wave eventually causes a full reversal of the flow at the exhaust outlet with ambient air drawn in behind the hot exhaust gases. The rarefaction wave is then reflected at the exhaust outlet as a weak compression wave, seen in Fig. 8.

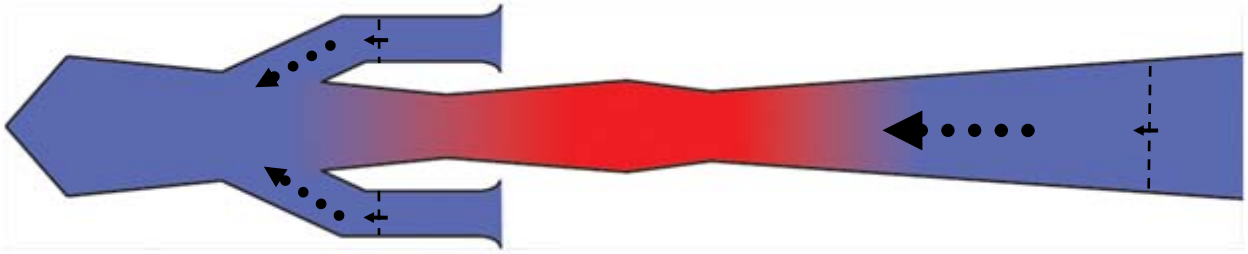

Figure 8. Reflection of Compression Wave

When the compression wave reaches the combustion chamber, the inflow of fresh air is momentarily slowed enough to allow for combustion to be initiated from the hot exhaust gases that are now flowing back into the combustion chamber, as shown in Fig. 9.

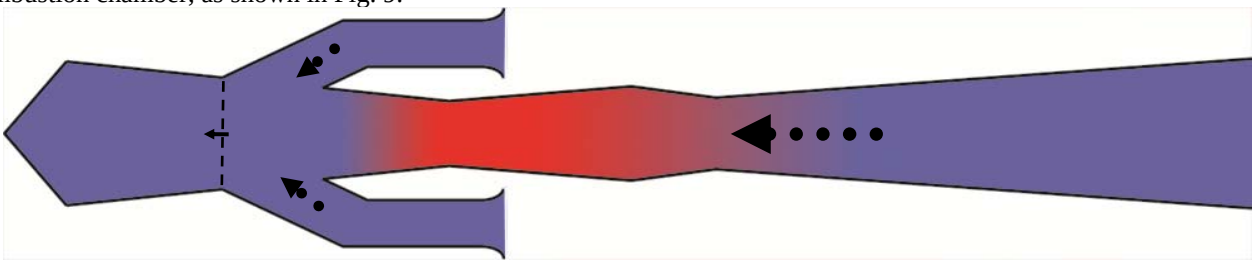

Figure 9. Compression Wave Slows Flow to Restart Combustion Cycle

The cycle is then repeated.

D. Theory

The two most popular theories to describe the pulsejet engine cycle are the Kadenacy Effect and acoustical resonance. While more than likely both are occurring, only the Kadenacy Effect is described in the preceding Operating Principle section.

The Kadenacy Effect describes the movement of the gases through pressure waves and the inertia of these gases. It is important to note that the pressure waves, compression and rarefaction, move through the ducts at the speed of sound independent of air masses themselves. This should not be taken to mean that the pressure waves do not affect the air masses as they certainly due as will be shown later. It should also be noted that the speed of sound, Mach 1, is faster in a pulsejet than the ambient speed of sound due to the high temperatures.[4]

The Kadenacy Effect was first discovered by the Dutch physical scientist Christiaan Huygens in the 1600s but got its name from the physicist Michael Kadenacy who studied it in the 1930s. He found when studying two stroke engines that the momentum of the exhaust gases leaving the cylinder will assist in the suction of fresh air into that same cylinder. What occurs is when high pressure air is allowed to quickly leave a rigid pressure vessel though a large opening the pressure inside the vessel drops to ambient but the inertia of the out flowing gas continues to draw air out of the reservoir. This causes the air pressure inside to continue to fall. In the absolute sense, this negative pressure eventually stops the outflow and now the reversed pressure differential draws air back into the reservoir to refill it. The same event occurs in the opposite direction and the momentum of the inflowing air brings the internal pressure of the vessel to above ambient and the cycle starts over. This effect eventually damps out due to losses of friction drag, and turbulence.

Looking at this more closely, when deflagration occurs the high pressure compression wave travels down the ducts. With a reference frame that holds the pressure wave stationary and taking a control volume of air at the rise of the compression pressure wave one can see the pressure differential imparted on the fluid, as shown in Fig. 10.[4]

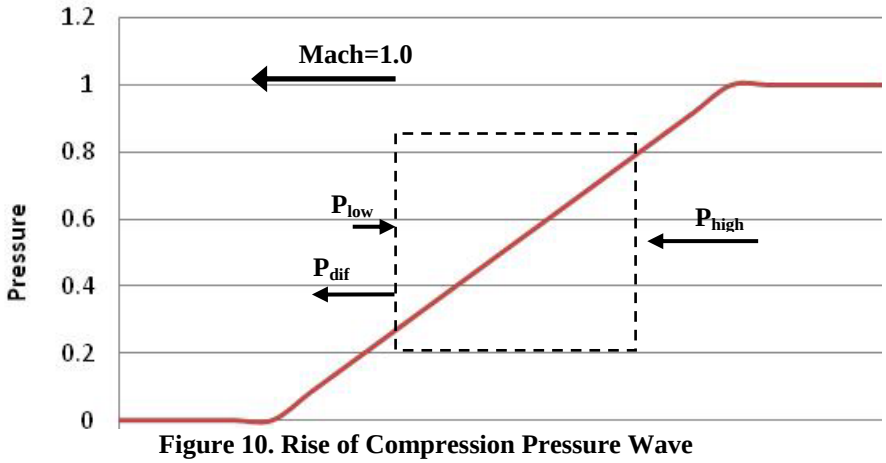

Figure 10. Rise of Compression Pressure Wave

The pressure differential acts to accelerate the flow since

$$F = P_{dif} \cdot A \tag{1}$$

$$a_1 = \frac{F}{m} \tag{2}$$

This pushes the air mass in the same direction as the pressure wave.

Holding the reference frame now at the trailing end of the compression wave, Fig. 11 shows that the opposite pressure differential decelerates to flow back to its original state.

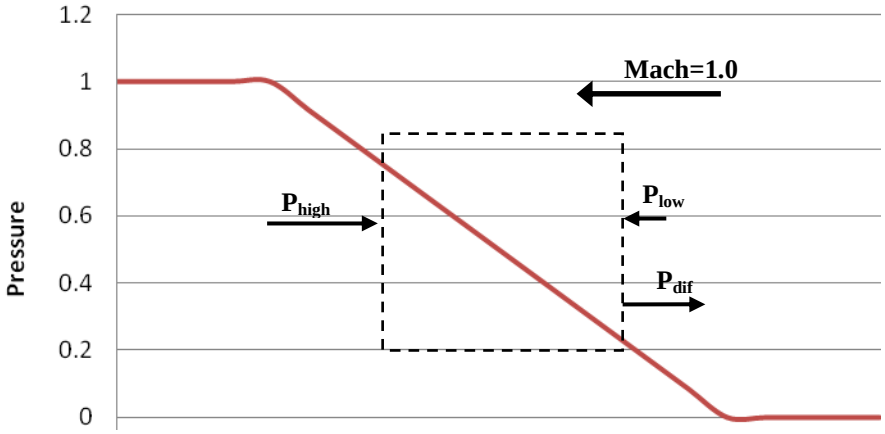

Figure 11. Loss of Compression Pressure Wave

$$a_2 = \frac{-P_{dif} \cdot A}{m} \tag{3}$$

$$a_1 + a_2 = 0 \tag{4}$$

The sum of the two accelerations is equal to zero. This does not return the air mass to the original position, only the original speed so a net forward movement in the direction of the compression wave has been imparted on the air mass.

When the compression pressure wave is reflected as a low pressure rarefaction wave it is in the absolute sense a negative pressure differential. Taking the same reference frame with the low pressure wave, Fig. 12 shows that the pressure differential points opposite the movement of the wave.

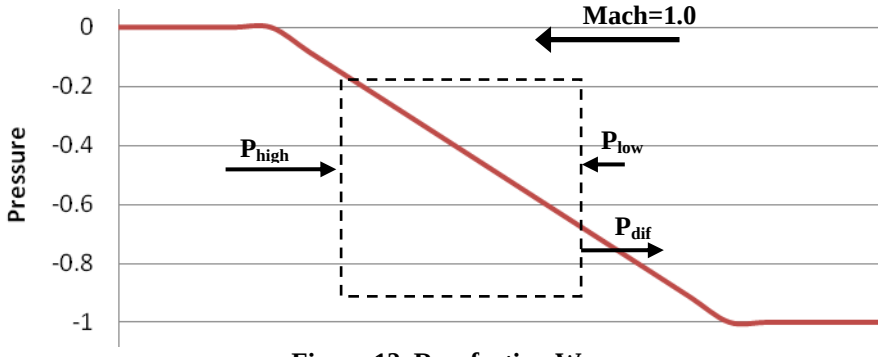

Figure 12. Rarefaction Wave

The lower pressure also causes a decrease in density and increase in volume inside the rarefaction wave. Like the compression wave when the rarefaction wave trailing edge passes, the net acceleration goes to zero and the air mass returns to its previous speed.

Overall this shows that while the hot gases of combustion are expanding and flowing out the ducts, the compression and rarefaction waves travel through the air mass helping it along in the desired direction for each part of the cycle.

The acoustic resonance theories explain the same process another way; when deflagration occurs in the combustion chamber pressure waves travel up and down the duct reflecting off the open and closed ends of the tube. These reflections meet and form a standing wave.

The combustion chamber has the least gas movement but the pressure changes here are the greatest. This makes it a speed node and a pressure antinode. The open ends of the intake and exhaust have the most gas movement but the least pressure differential as the pressure is constant atmospheric.[1]

The smallest wave a resonating vessel can accommodate is a quarter of a wavelength. For a pulsejet a quarter of a wavelength will span the pressure antinode in the combustion chamber and the pressure node at the exhaust opening. This length will also determine the fundamental wavelength of the standing wave that will govern the engine. The distance between the intake opening and the combustion chamber is much shorter and will accommodate a quarter of a shorter wavelength. This secondary wavelength is an odd harmonic of the fundamental.

Normally, open tube resonators carry half a wavelength, a pressure antinode in the center and nodes at each end but it is closer to reality to model a valveless pulsejet as two quarter wave oscillators mounted back to back.

The operating principle section only describes the Kadenacy Effect but both the Kadenacy Effect and acoustical resonance do occur. An efficient pulsejet would harness the positive effects of resonant frequencies.

III. Design

The valveless pulsejet design that was chosen is the Focused Wave Engine (FWE) VIII Twin Stack. This design was chosen for its small scale, low thrust, and potential for UAV application.

The design is a modification by Graham Williams and James D of a design by Larry Cottrill of Cottrill Cyclodyne Corporation.

Blueprints are shown on the next page.

FWE VIII Twin Stack REV08

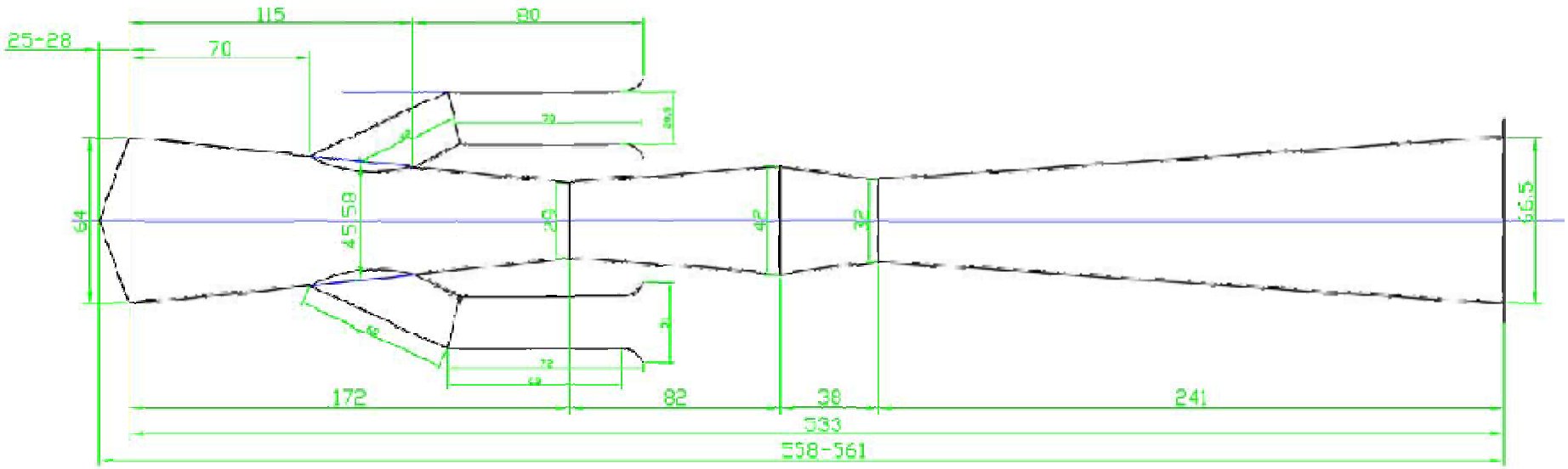

Do Not Scale

All dimensions: Internal mm

This Drawing: Graham C. Williams 2008

IV. Manufacture

The material of choice for pulsejets is stainless steel due to its rust and corrosion resistance. Both of these occur at an accelerated rate at the high operating temperatures. The entire pulsejet is formed from thin sheet metal which is cut and rolled into tubes and cones. Manufacturing was preceded by solid modeling the pulsejet in SolidWorks. This was done using SolidWorks sheet metal tools to allow for the generation of flat patterns to be used as a template for the sheet metal. The flat patterns are provided in the appendix with a 5mm tab to allow overlapping of the edges. The SolidWorks model is shown in Figure 13.

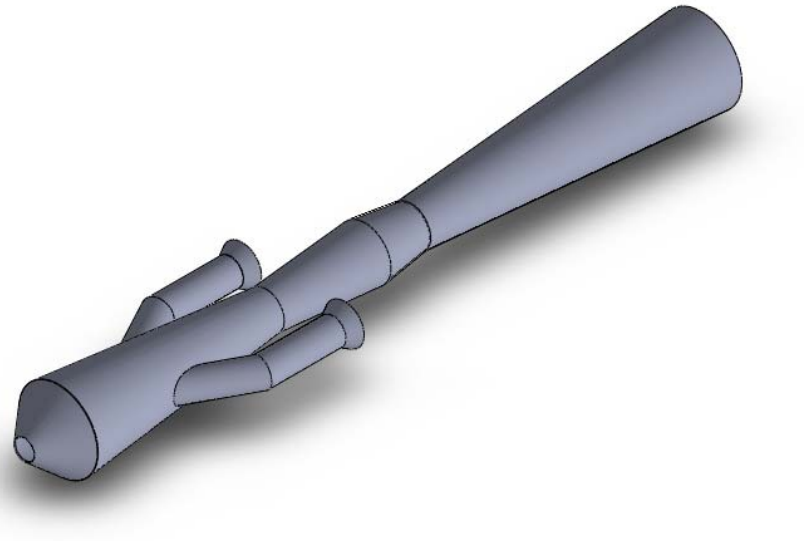

Figure 13. Isometric View of SolidWorks Model

Using the flat patterns and an optically-driven plasma cutter the rough shapes were easily cut. From there the pieces were finish ground to the final size.

Many difficulties were faced during the construction of the pulsejet such as rolling the flat sheet metal into cones and welding. The paper mockup utilizing the cut out paper templates and tape did not portray the challenges of forming the sheet metal but did verify that all pieces would fit correctly. The smallest sheet metal roller found on campus has inch and half rollers while the smallest diameter of the cones is around three quarters of an inch. This could be used to start shaping the pieces but was a balancing act to keep friction in order to drive the piece through the machine and having it loose enough in order to rotate the piece. It is necessary to rotate the piece in order to form a cone and not a tube. The best method that was found to finish the pieces used a steel pipe clamped to a workbench with a small gap just larger than the thickness of the sheet metal in order to fit the sheet between the pipe and the bench. The sheet could then be hand bent using leather gloves or a hammer using a large amount of small bends repositioning the piece each time to travel from one edge to the other. Once this process was complete and the cones were rolled, the individual cones were TIG welded along the seam and then together end to end. With no experience TIG welding sheet metal the process had a learning curve but was made easier by using a steel backing bar behind the seam to be welded and the 5mm overlap creating a lap weld instead of a butt weld.

The inlet tubes were made in the previous fashion and then were to be flared. Unfortunately their 20.5mm inside diameter made them larger than would fit in a standard 3/4" flaring tool. Applied heat and working using a spinning type setup on the lathe was attempted with little success. A die was machined and attempted to be pressed into the tube in order to flare it but the intense strain cracked the inlet tube along the flare. It was eventually determined to roll the flare as a separate “cone” as with the rest of the motor and weld it on to the end of the straight section.

The finished pulsejet is pictured in Figure 14.

Figure 14. Completed FWEVIII Pulsejet Engine

The materials and pricing for manufacturing and testing of the pulsejet are tabulated in Table 1.

Table 1. Materials Invoice

Item Description	Unit Price	Total Price
Pulsejet		
Stainless Steel , 20 ga, 18”x18”		$45 +tax
4mm copper tubing	~$2	$10
Sparkplug	~$2	$2
Auto Ignition Coil	~ $15	$15
Fuel Line Fittings	~$4	$20
Ignition Circuit		Provided
Car Battery		Provided
Propane Tank		Provided
Propane regulator		Provided
Stand		
Steel		$15
Instrumentation		
Load Cell		Provided
	TOTAL	$107

V. Testing Apparatus and Procedure

The testing apparatus for the pulsejet design had to accomplish three things in order to properly run the engine. First, it had to be able to inject propane fuel and pressurized air into the inlets of the pulsejet. This was accomplished by connecting 0.25” outside diameter copper tubing from a propane tank into the inlets of the pulsejet. For the pressurized air, a copper tube was connected to an air hose and manually placed within the inlet, allowing the tester to move the air hose around to find the optimum location for the fuel and air to mix.

The test stand also had to have a way of igniting the fuel in the combustion chamber. This was done by attaching a standard spark plug to the nose of the pulsejet. This spark plug was then connected to a 12 volt DC 215 amp Bendix Aircraft starting vibrator and a high voltage Ford ignition coil, resulting in the necessary sparks for combustion. The vibrator and ignition coil were connected to a 12 volt car battery to power the ignition system. Additionally ground wires were connected between the spark plug and the vibrator. A picture of the test stand setup is shown in Figure 15.

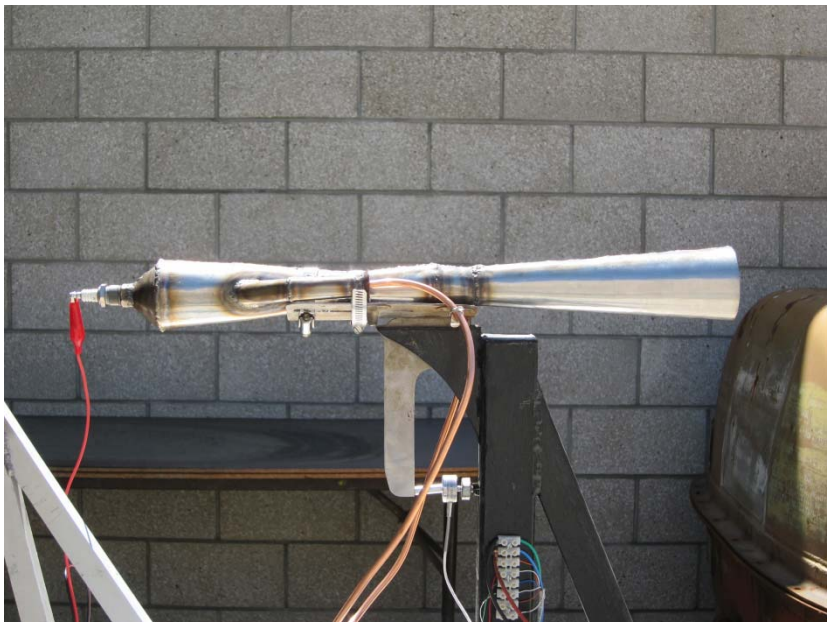

Figure 15. Pulsejet Test Stand

The final aspect of the test stand was data acquisition. The pulsejet was connected to a stand that would push on an Omegadyne LCFD-25 load cell once thrust was produced. This load cell was then connected to a National Instruments NIUSB-6008 DAC which fed the data into a LabView program to measure the thrust of the pulsejet.

In order to best protect the operators during the testing of the pulsejet, several safety measures were taken. Only one person was in the room during operation; behind a blast shield to avoid any danger. The other person was in the test room, behind a thick panel of glass. Both researchers wore ear muffs and the researcher in the room with the engine was wearing protective safety goggles and gloves. The line from the propane to the intake was checked for leaks before any experimental runs.

Before the testing of the pulsejet began, the load cell was calibrated with weights between 250g and 1500g at intervals of 250g. The procedure for running the pulsejet and collecting thrust data required one experimenter to be running the propane and air hose while the other had control of the ignition switch and the data acquisition computer. The test is started by turning on the ignition switch, followed by opening the propane valve and then blowing pressurized air across one of the inlets. The fuel and air will combust soon after that, and the air hose is positioned to allow the pulsejet to begin its pulsing cycles. At this point the combustion chamber will begin to glow a bright orange, signaling that the air hose can be removed from the inlets and the ignition switch can be turned off. Then the wires connecting the vibrator to the spark plug are removed and the data acquisition begins. During the tests the propane valve was opened up to simulate a throttling up of the engine. To turn off the pulsejet, the propane valve was closed and the pulsejet was allowed to cool off for several minutes. The pulsejet is shown running in Figure 16.

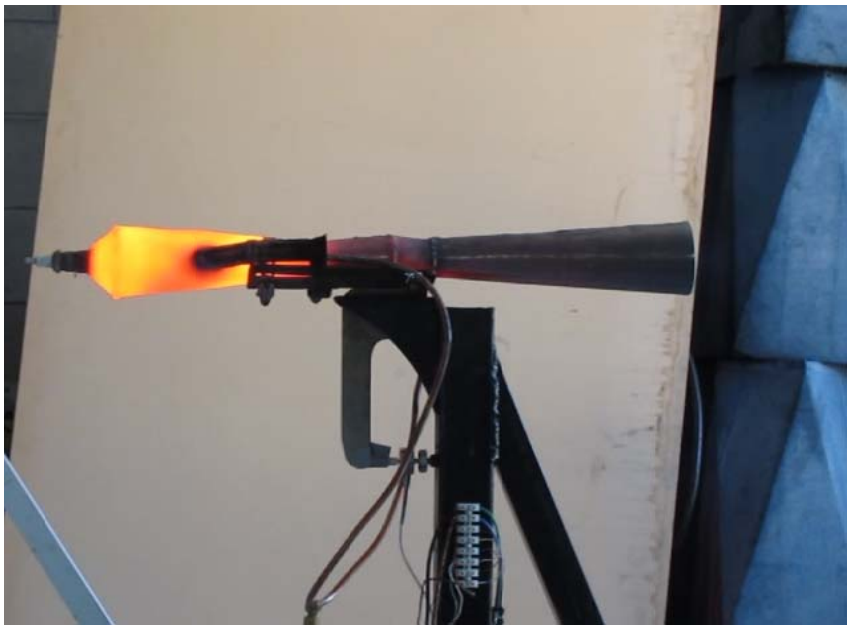

Figure 16. Running Pulsejet Engine

VI. Results and Discussion

Thrust was measured via the load cells discussed in the previous section, from the time the spark plug wires were disconnected to several seconds after pulsing had stopped within the pulsejet. The data acquisition was originally very noisy, so an exponentially weighted moving average was used to make it possible to see how the thrust changed with throttling. Figure 17 shows the results of the first of two test runs. There is a slight increase in thrust at approximately the 15 second mark, where the engine is being throttled up. After that the engine is continuously throttled up, and moves beyond the optimum fuel to air ratio, which decreases the thrust performance. Eventually, at the 37 second mark there is too much fuel when compared to air and the pulsing stops, resulting in no more thrust. At an optimum fuel to air ratio, the pulse jet produces on average 4.5 lbs of thrust.

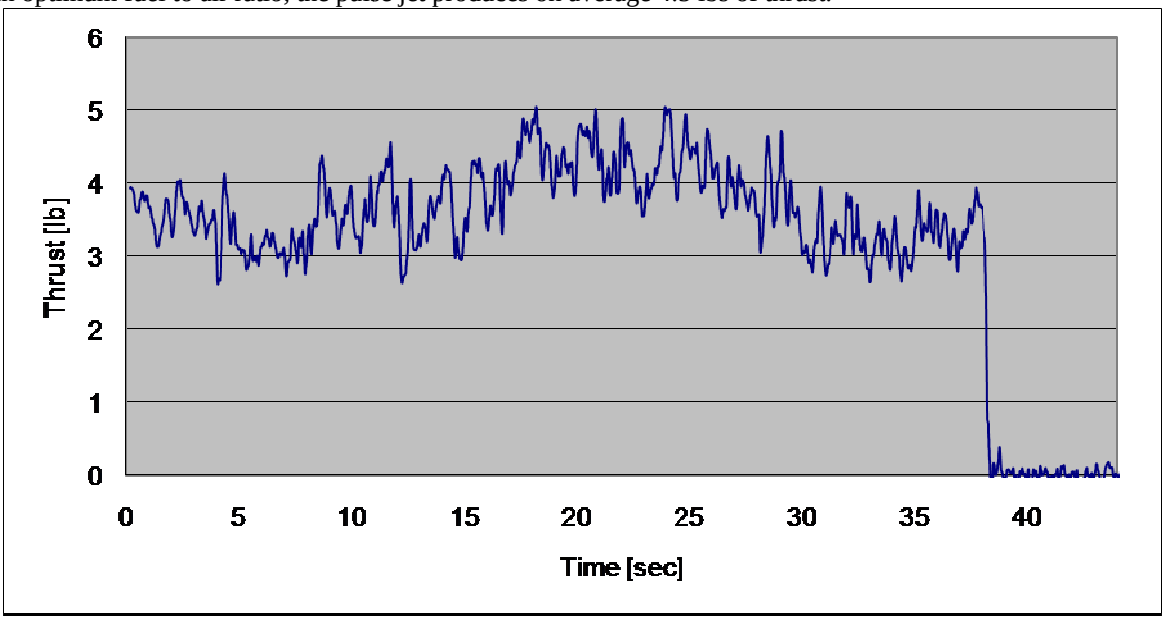

Figure 17. Thrust trace of the pulsejet engine, first run.

Figure 18 represents the second run of the pulsejet, where the engine was throttled to the optimum fuel to air ratio much earlier in the test. Afterwards, the engine settles into a somewhat steady value of about 2.5 lbs of thrust before the propane was shut off.

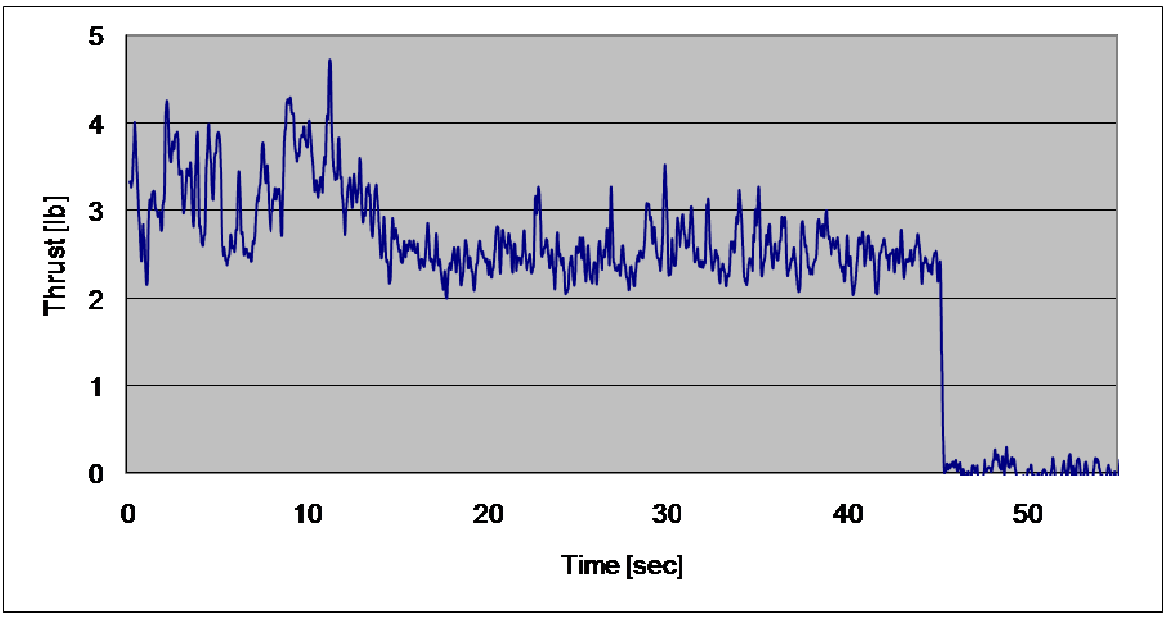

Figure 18. Thrust trace of the pulsejet engine, second run.

However, there is a limit to the amount of information that can be obtained from these thrust measurements. The load cell and DAC being used for this experiment were using sample frequencies of 1 kHz but only returned data at 250 Hz due to limitations of the load cell. The engine has a running frequency of 150 Hz and produces harmonic frequencies at 1.5 kHz, requiring that we would need a sample frequency upwards of 10 kHz to be able to accurately track the actual pulsating that is going on with the engine thrust. This would require moving up to a dynamic load cell that is too costly for the scope of this senior project.

This also means that the pulsating that seems to be occurring in Figure 17 and Figure 18 is only capturing a portion of the thrust pulsing that is actually occurring. Since not enough data samples are being taking, it is impossible to accurately conclude that the pulsing of the pulsejet would look anything like the results presented. Due to this fact, the goal of the thrust traces is to get a feel for an average of the thrust being produced by the pulsejet, not the actual pulsing that is physically going on.

VII. Future Research

In order to further improve on the pulsejet research, several things can be done during the testing phase that would enhance the results. A pressure transducer that measures a pressure differential of 30 psi which would be compared with theoretical results to see how close to optimum the pulsejet is performing. Additionally, further research in the effects of optimum fuel to air ratios and maximizing flow into the inlets could potentially show improvements in thrust and efficiency within the engine. Finally, tests could be done to see the effect of different fuels on the pulsejet. Potentially something such as gasoline or Jet A fuel could be an alternate fuel source to the pulse jet and with acceptable fuel injection, these fuels could allow for greater thrust from the engine and overall lighter setup that could be used on a unmanned air vehicle or RC plane.

References

[1]Ogorelec, B., "Valveless Pulsejet Engines 1.5," http://www.pulse-jets.com/valveless/, [accessed: 3/14/09]

[2]Anderson, R., Lukacs, N., O'Callaghan, M., Schumacher, K., Sipols, M., Walladge, T., "Design and Build of a Pulsejet UAV," School of Mechanical Engineering, University of Adelaide, Adelaide, Australia, 2006.

[3]Sulprizio, C., "Lockwood Valveless Pulsejet," Senior Project, Mechanical Engineering Dept., Cal Poly Univ., San Luis Obispo, CA, 2003.

[4]Cottrill, L., "First Principles: The Kadenacy Effect," http://jetzilla.com/topic_003_01.html, [accessed: 3/14/09]

[5]Blair, G. P., Artt, D. W., and Richardson, J. S., "A Computer Model of a Pulsejet Engine," SAE 820953, 1982.

Appendix

The following pages contain the paper templates used. All have a 5mm tab on one edge even if they are not marked with a line separating it from the main part. If using the templates, be sure to print with no scaling.

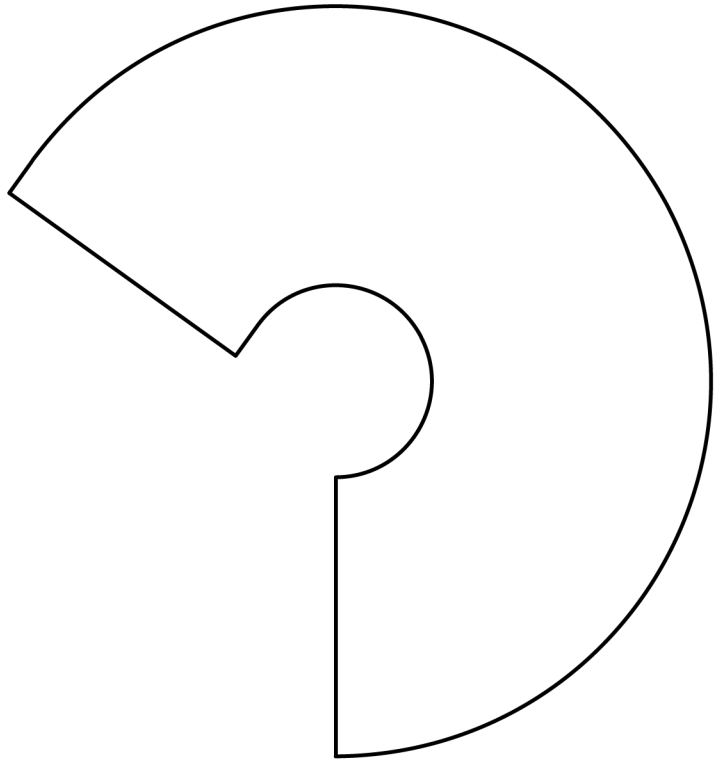

		UNLESS OTHERWISE SPECIFIED:		NAME	DATE
		DIMENSIONS ARE IN INCHES TOLERANCES: FRACTIONAL ± ANGULAR: MACH ± BEND ± TWO PLACE DECIMAL ± THREE PLACE DECIMAL ±	DRAWN		
			CHECKED		
			ENG APPR.		
			MFG APPR.		
		INTERPRET GEOMETRIC TOLERANCING PER:	Q.A.		
		MATERIAL	COMMENTS:		
NEXT ASSY	USED ON	FINISH			
APPLICATION		DO NOT SCALE DRAWING			

TITLE:

SIZE	DWG. NO.	REV
A	nose	
SCALE: 1:1	WEIGHT:	SHEET 1 OF 1

5 4 3 2 1

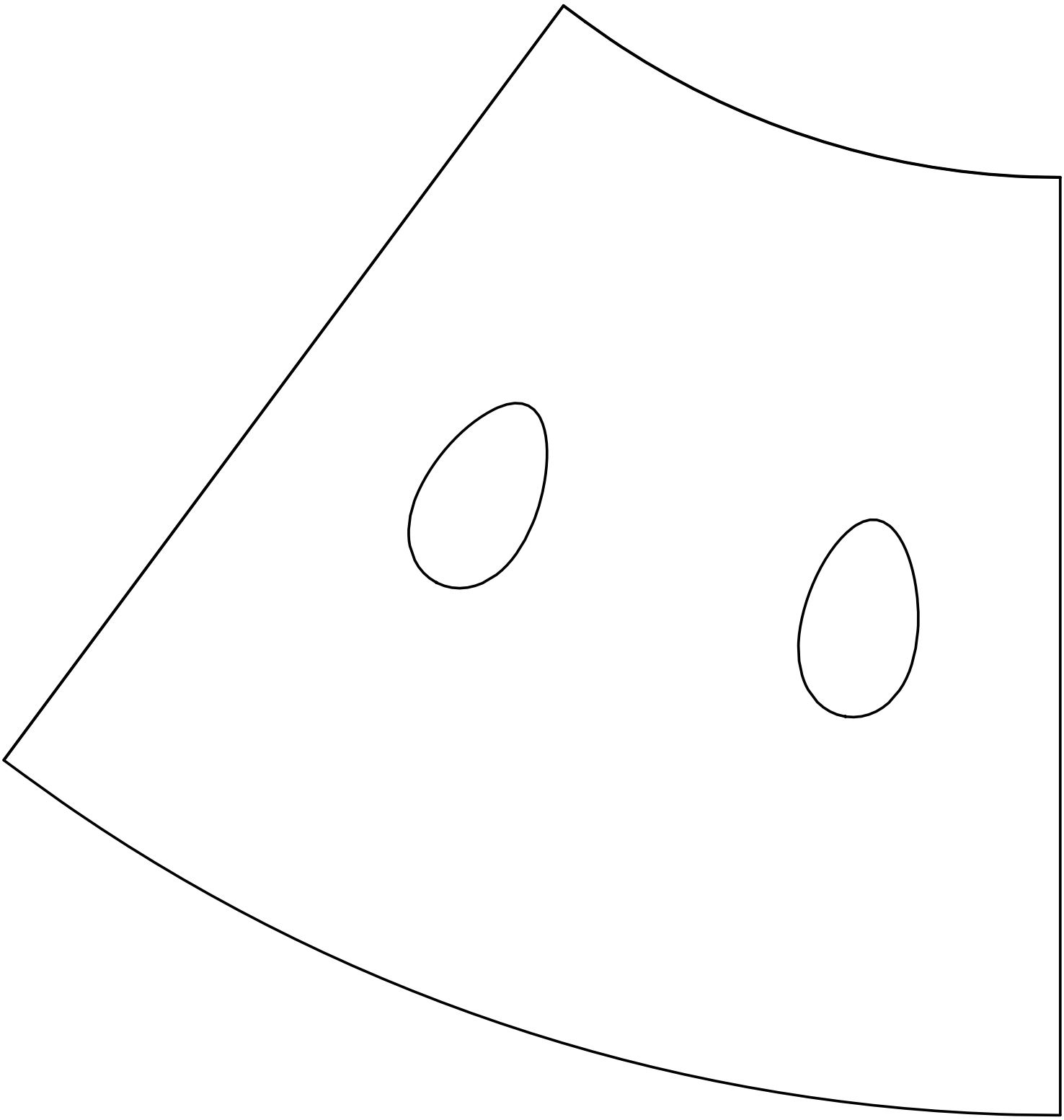

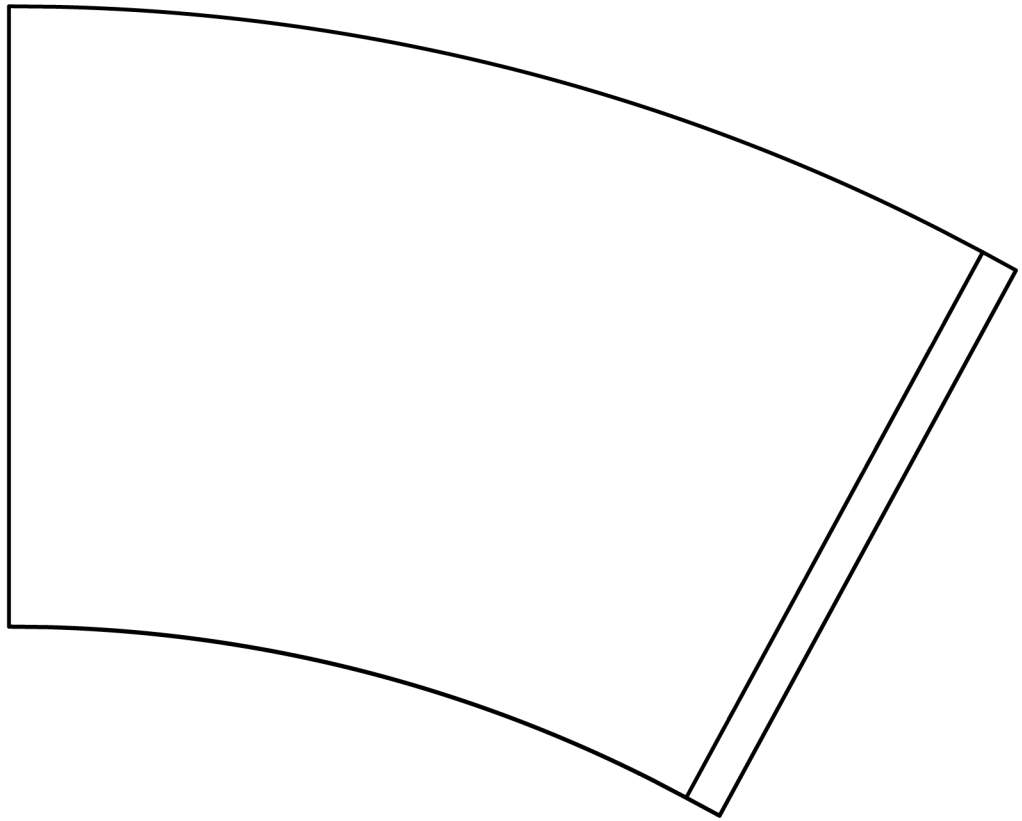

		UNLESS OTHERWISE SPECIFIED:		NAME	DATE
		DIMENSIONS ARE IN INCHES TOLERANCES: FRACTIONAL ± ANGULAR: MACH ± BEND ± TWO PLACE DECIMAL ± THREE PLACE DECIMAL ±	DRAWN		
			CHECKED		
			ENG APPR.		
			MFG APPR.		
		INTERPRET GEOMETRIC TOLERANCING PER:	Q.A.		
		MATERIAL	COMMENTS:		
NEXT ASSY	USED ON	FINISH			
APPLICATION		DO NOT SCALE DRAWING			

TITLE:

SIZE	DWG. NO.	REV
A	exhuast1	

SCALE: 1:1	WEIGHT:	SHEET 1 OF 1

5 4 3 2 1

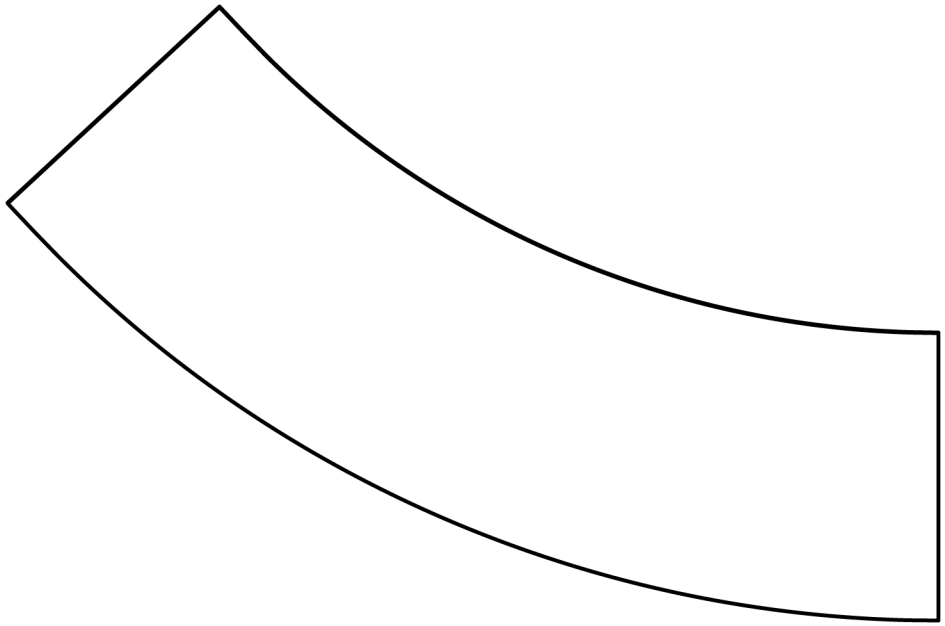

		UNLESS OTHERWISE SPECIFIED:		NAME	DATE
		DIMENSIONS ARE IN INCHES TOLERANCES: FRACTIONAL ± ANGULAR: MACH ± BEND ± TWO PLACE DECIMAL ± THREE PLACE DECIMAL ±	DRAWN		
			CHECKED		
			ENG APPR.		
			MFG APPR.		
		INTERPRET GEOMETRIC TOLERANCING PER:	Q.A.		
		MATERIAL	COMMENTS:		
NEXT ASSY	USED ON	FINISH			
APPLICATION		DO NOT SCALE DRAWING			

TITLE:

SIZE	DWG. NO.	REV
A	exhaust 2	

SCALE: 1:1	WEIGHT:	SHEET 1 OF 1

5 4 3 2 1

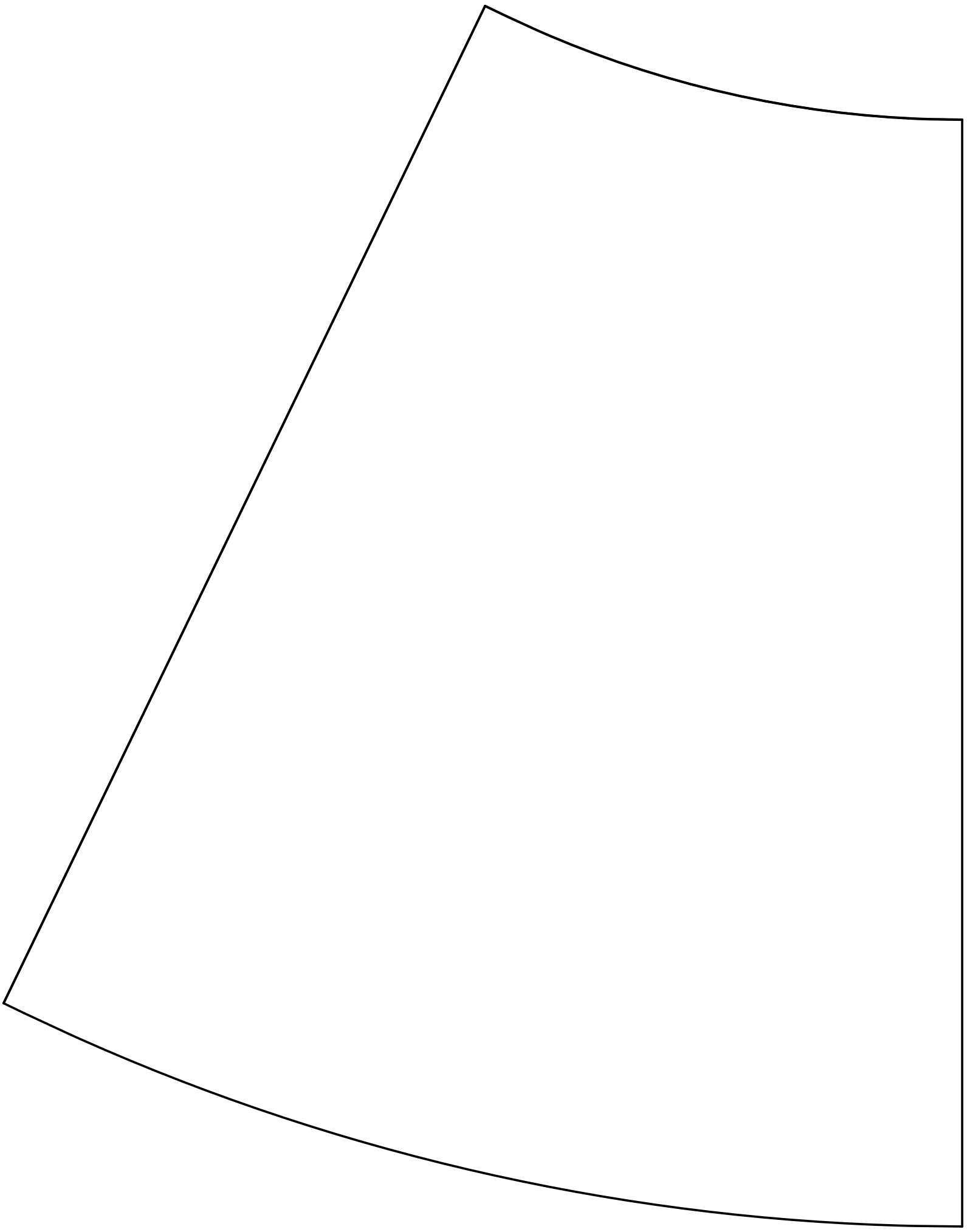

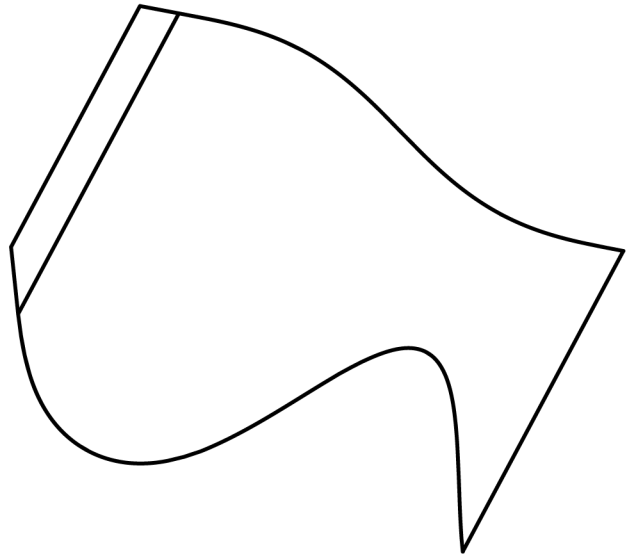

Require two

		UNLESS OTHERWISE SPECIFIED:		NAME	DATE
		DIMENSIONS ARE IN INCHES TOLERANCES: FRACTIONAL ± ANGULAR: MACH ± BEND ± TWO PLACE DECIMAL ± THREE PLACE DECIMAL ±	DRAWN		
			CHECKED		
			ENG APPR.		
			MFG APPR.		
		INTERPRET GEOMETRIC TOLERANCING PER:	Q.A.		
		MATERIAL	COMMENTS:		
NEXT ASSY	USED ON	FINISH			
APPLICATION		DO NOT SCALE DRAWING			

TITLE:

SIZE	DWG. NO.	REV
A	intake1	
SCALE: 1:1	WEIGHT:	SHEET 1 OF 1

5 4 3 2 1

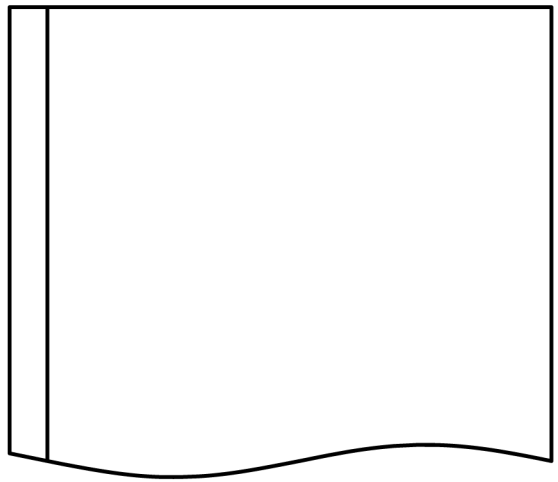

Require two

		UNLESS OTHERWISE SPECIFIED:		NAME	DATE
		DIMENSIONS ARE IN INCHES TOLERANCES: FRACTIONAL ± ANGULAR: MACH ± BEND ± TWO PLACE DECIMAL ± THREE PLACE DECIMAL ±	DRAWN		
			CHECKED		
			ENG APPR.		
			MFG APPR.		
		INTERPRET GEOMETRIC TOLERANCING PER:	Q.A.		
		MATERIAL	COMMENTS:		
NEXT ASSY	USED ON	FINISH			
APPLICATION		DO NOT SCALE DRAWING			

TITLE:

SIZE	DWG. NO.	REV
A	Intake2	
SCALE: 1:1	WEIGHT:	SHEET 1 OF 1

5 4 3 2 1

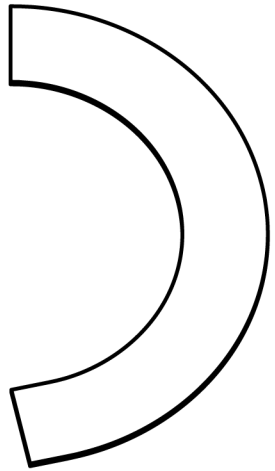

Require two

		UNLESS OTHERWISE SPECIFIED:		NAME	DATE
		DIMENSIONS ARE IN INCHES TOLERANCES: FRACTIONAL ± ANGULAR: MACH ± BEND ± TWO PLACE DECIMAL ± THREE PLACE DECIMAL ±	DRAWN		
			CHECKED		
			ENG APPR.		
			MFG APPR.		
		INTERPRET GEOMETRIC TOLERANCING PER:	Q.A.		
		MATERIAL	COMMENTS:		
NEXT ASSY	USED ON	FINISH			
APPLICATION		DO NOT SCALE DRAWING			

TITLE:

SIZE	DWG. NO.	REV
A	Intake3	
SCALE: 1:1	WEIGHT:	SHEET 1 OF 1

5 4 3 2 1